MONTE-CARLO ANALYSIS OF MINIMUM THERMOCOUPLE DEPTHS USING ICARUS

THERMAL AND FLUIDS ANALYSIS WORKSHOP 2022

Joseph Schulz
Analytical Mechanics Associates, Inc.
NASA Ames Research Center
Moffett Field, CA

September 6, 2022

ABSTRACT

Icarus is a three-dimensional, unstructured, finite-volume material response solver developed at NASA Ames Research Center Schulz et al. [2017] and has been verified against other NASA material response tools like FIAT, which have a long history of successfully designing thermal protection system (TPS). Icarus solves a set of conservation equations for mass and energy and uses Darcy's Law in place of momentum conservation. An ecosystem of material response tools has been built around a general-purposed Icarus library that in addition to the typical material response analysis also supports TPS sizing (1-D and multi-dimensional), uncertainty quantification, and has been successfully integrated into a multi-physics architecture built around US3D Schroeder et al. [2021]. In this paper, a brief overview of Icarus and its capabilities will be presented using an illustrative Monte Carlo analysis of the one-dimensional, in-depth material response of a representative Dragonfly trajectory.

1 Introduction

As a part of the New Frontiers program, Dragonfly is a rotorcraft/lander mission that will explore Titan. In addition to the planned two-year mission on Titan, Dragonfly will be the first mission equipped with instrumentation to provide key aerothermodynamic data during its entry and descent through Titan's atmosphere. In partnership with NASA Ames Research Center, NASA Langley Research Center, and DLR, the instrumentation suite known as Dragonfly Entry Aerosciences Measurements (DrEAM) Brandis et al. [2022], Santos et al. [2021] will use a sensor systems similar to the Mars Entry, Descent, and Landing Instrumentation 2 (MEDLI2) Instrumented Sensor Plug (MISP) and the COMbined Aerothermal and Radiometer Sensor (COMARS) suite Hwang et al. [2013]. For DrEAM, the MISP-heritage plugs will be known as Dragonfly Sensors for Aero-Thermal Reconstruction (DragSTR) plugs. Each plug will consist of 1 to 3 thermocouples embedded at different depths within a cylindrical piece of material that matches the TPS material (PICA on the heatshield and SLA 561V on backshell) and is flush-mounted in the aeroshell. Nominally, five plugs are planned to be installed across the heatshield, and a single plug will be installed on the backshell Santos et al. [2021]. Since the details of the aeroshell TPS design are still being iterated, only a preliminary layout of the sensors is known at this time. More specifically, the number, depths, and types of thermocouples to use in each DragSTR plug is still under consideration.

The temperatures measured at each DragSTR plug during Dragonfly entry will be used to reconstruct the aerothermal heating environment at those locations by solving an inverse material response problem (see Bose et al. [2013] and Alpert et al. [2022] for more details about MEDLI and MEDLI2 flight reconstructions). More specifically, the inverse problem is posed as an optimization problem that determines the surface heating required to minimize the difference between the predicted in-depth temperature from a material response model and the DragSTR temperature data. The thermocouple depth affects the predictive capability of the surface heating reconstructions. First, temperature data measured from locations closer to the surface are more sensitive to surface heating making the inverse problem

easier to solve and time-sensitive events easier to predict accurately, such as laminar-to-turbulent transition (a level 1 requirement for DrEAM). Second, as the thermocouple depth is increased the temperature data is increasingly affected by uncertainties in the material properties and deficiencies in the material response model. These two considerations are bound by the maximum allowable temperature at which the thermocouple can be exposed to in order to avoid loss of data. Thermocouple burn-out can be mitigated by embedding multiple thermocouples at different depths within each DragSTR plug; however, the total number of thermocouples are limited by the amount of data available to the sensor system. As a preliminary study to determine the optimum thermocouple depth appropriate for each DragSTR plug, a Monte Carlo analysis is performed to determine the sensitivity of the in-depth temperature based on the temperature limitations of R-type (1750 K) and K-type (1530 K) thermocouples (TCs).

For MEDLI2, the near-surface TC in each heatshield MISP is R-type, while the deeper TCs and all TCs in each backshell MISPs were K-type Hwang et al. [2013]. For surface heating reconstruction, only data from the near-surface TCs were used, and all near-surface TCs were nominally installed at either 0.075 in (1.91 mm) or 0.1 in (2.54 mm) beneath the surface. None of the TCs failed, and the temperature recorded by any of the TCs never exceeded the limits of the R-type TCs on the heatshield or the K-type TCs on the backshell. Since the heatshield was coated by NuSil, the oxidization of the PICA surface was minimized reducing the expected recession. As a result, the inverse analysis preformed on the MEDLI2 data did not consider recession in the surface energy balance boundary condition (more detailed provided below) used by the material response model Alpert et al. [2022] . For Dragonfly, a NuSil coating may be similarly applied, but since oxidization will not occur at Titan, material recession of the heatshield surface is not expected.

2 Material Response Modeling

Icarus is a three-dimensional, unstructured, finite-volume material response solver developed at NASA Ames Research Center Schulz et al. [2017] and has been verified against other NASA material response tools like FIAT, which have a long history of successfully designing thermal protection system (TPS). Icarus solves a set of conservation equations for mass and energy, while using Darcy's Law to reduce the equation for momentum conservation to an equation for the velocity of the pyrolysis gas mixture as a function of the local pressure gradient and permeability,

$$u_{g,i} = -\frac{K_{ij}}{\phi\mu}\frac{\partial p}{\partial x_j} \tag{1}$$

where μ is the viscosity of the pyrolysis gas mixture, ϕ is the porosity of the material, p is the pressure, and K_{ij} is the permeability tensor, which can be either isotropic (in which the permeability is a scalar) or transversely isotropic (in which the permeability is defined by a transverse or through-the-thickness component and an in-plane component). Both thermal and chemical equilibrium is assumed. Thus, the state of the pyrolysis gas mixture is uniquely defined by the pressure and temperature, p and T. The total energy is then given as

$$\rho e = \phi\rho_g e_g + \rho_s e_s = \phi\rho_g e_g + \left(\sum_{n=1}^{N_s}\Gamma_n\rho_{s,n}\right)e_s, \tag{2}$$

where Γ_n and $\rho_{s,n}$ are the pseudo-volume fraction and densities of the n^{th} material component, respectively, $\rho = \phi\rho_g + \rho_s$ is the total density, e_g is the internal energy of the equilibrium pyrolysis gas mixture, and e_s is the total internal energy of the material. The number of material components, N_s, depends on the chosen decomposition model. For example, in a widely used three-component decomposition model for porous ablators Moyer and Rindal [1968], the phenolic resin undergoes a two-stage decomposition process, and the binder composite undergoes a single-stage decomposition. The pressure, temperature, and density are related through the perfect gas equation of state,

$$p = \rho_g\left(\frac{\mathcal{R}}{W_g}\right)T = \rho_g R_g T. \tag{3}$$

where W_g is the molecular weight of the pyrolysis gas mixture, and R_g is the respective gas constant.The complete set of conservation equations is given by

$$\frac{\partial\rho_{s,n}}{\partial t} = \dot{\omega}_{s,n} \tag{4}$$

$$\frac{\partial(\phi\rho_g)}{\partial t} - \frac{\partial}{\partial x_i}\left[\left(\frac{K_{ij}}{\mu}\right)\rho_g\frac{\partial p}{\partial x_j}\right] = \dot{\omega}_g, \tag{5}$$

$$\frac{\partial(\rho e)}{\partial t} - \frac{\partial}{\partial x_i}\left[\left(\frac{K_{ij}}{\mu}\right)\rho_g h_g\frac{\partial p}{\partial x_j}\right] - \frac{\partial}{\partial x_i}\left(\kappa_{ij}\frac{\partial T}{\partial x_j}\right) = 0. \tag{6}$$

where k_{ij} is the thermal conductivity tensor (similar to the permeability many porous materials are anisotropic), h_g is the enthalpy of the pyrolysis gas mixture, and the rates of decomposition and the production of the pyrolysis gas mixture are given by

$$\dot{\omega}_{s,n} = -k_n \rho_{v,n} \left(\frac{\rho_n - \rho_{c,n}}{\rho_{v,n}} \right)^{\psi_n} \mathrm{e}^{(-T_{a,n}/T)}, \tag{7}$$

$$\dot{\omega}_g = - \sum_{n=1,N_s} \Gamma_n \dot{\omega}_{s,n}, \tag{8}$$

A three-component decomposition model is used in the present study. Thus, the bulk solid density is represented by two components of the phenolic resin with virgin and char densities of $\rho_{v/c,1}$ and $\rho_{v/c,2}$ and a binder composite with virgin and char densities of $\rho_{v/c,3}$. The pseudo-volume fraction is 0.5 for all components. Amar et al. [2009]. It is important to note that the notion of three distinguishable species is an artifact of the model. Equation 8 states the assumption that all decomposed phenolic resin generates a pyrolysis gas mixture, which is further assumed to be thermal equilibrium with the material. A by-product of the decomposition model is that the material properties, k_{ij} and e_s, are defined as a linear combinations of their virgin ($k_{ij,v}$,$e_{s,v}$) and char ($k_{ij,c}$, $e_{s,c}$) values based on the mass fraction of virgin material, which is defined as

$$Y_v = \frac{\rho_v}{\rho_v - \rho_c} \left(1 - \frac{\rho_c}{\rho_s} \right). \tag{9}$$

The values ρ_v and ρ_c are the measured bulk densities of the solid virgin and solid product material or char, respectively. For example, the internal energy of the material would be determined by

$$e_s = Y_v e_{s,v} + (1 - Y_v) e_{s,c} \tag{10}$$

where both $e_{s,v}$ and $e_{s,c}$ are computed based on tabulated values of the specific heat as a function temperature. Similarly, the components of the thermal conductivity tensor of both the virgin and char are computed by interpolating tabular data provided as a function of temperature and pressure. The other material properties, ϕ and K_{ij}, are defined as functions of the extent of reaction,

$$\beta = \frac{\rho_v - \rho_s}{\rho_v - \rho_c} \tag{11}$$

The predictive capability of the above formulation depend on the many constituent relationships used to close the mass and energy conservation equations. Furthermore, boundary conditions (defined by the surface primitive state variables, ρ_s, p, and T) are needed to uniquely constrain the problem, which in turn introduce further assumptions. Paramount to the problem of TPS analysis is the coupled nature of material response simulations at the gas-material surface. Often a loosely-coupled approach is used where CFD solutions are computed for cold, unblown, and fully-catalytic surfaces Milos and Chen [2010]. Then, surface values for the pressure, recovery enthalpy, and cold-wall heat transfer coefficient are extracted from the CFD solutions and passed as boundary condition parameters to the material response model, which are then used to iteratively solve a surface energy balance for the primitive state variables, ρ_s, p, and T. Alternatively, (and the approach used here), the convective heat flux (rather than the recovery enthalpy and cold-wall heat transfer coefficient) is extracted from the CFD solution and passed to the material response model directly. Additional effects such as surface thermochemical interactions, blowing, and black-body radiation can be included in the surface energy balance as needed.

Since Titan's atmosphere is primarily composed of Nitrogen (about 95 percent) and methane, the TPS environment is expected to be non-oxidizing. As a result, PICA is not expected to undergo recession, which simplifies the surface energy balance used in the analysis of the Dragonfly heatshield to the following

$$q_s + \alpha q_{rad} - \sigma \epsilon \left(T^4 - T_\infty^4 \right) - q_{cond} = 0, \tag{12}$$

where q_s is the total convective heating, q_{rad} is the radiative heat flux, α and ϵ are the absorptivity and emissivity at the surface, T_∞ is the background temperature, σ is the Stefan-Boltzmann constant, and q_{cond} is the thermal conductive heat flux, which is a function of the temperature gradient and the thermal conductivity at the surface. Given a specified surface pressure, p_s, Equation 12 is iteratively solved for the temperature, which completes the specification of the boundary conditions for the conservation equations, Eqs. 4 - 6 (The conservation equations presented here also do not include terms accounting for the mass lost due to ablation since no recession is expected. The addition of these terms would require a mesh motion algorithm Schulz et al. [2017], which is turned off in the present study.) The values q_s, q_{rad}, T_∞, and p_s are determined from CFD solutions and provided as inputs to the material response solver. To construct a full time-history of the material response, a series of CFD simulations are used to generate temporal variations of these variables through the trajectory.

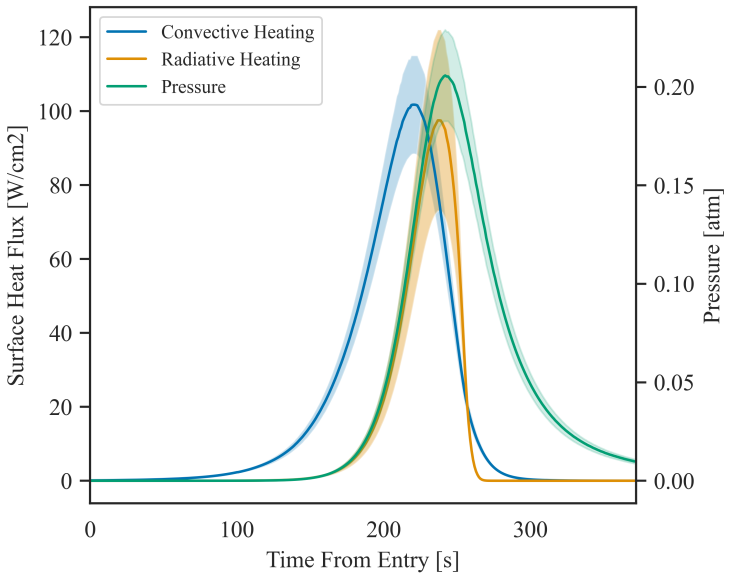

Figure 1: The nominal and margined aeroheating environments for Dragonfly entry are used to bound the uncertainty. Shaded regions show the distributions of the convective heat flux, radiative heat flux, and pressure at the stagnation point, and the solid lines show the mean values of each.

3 Monte Carlo Analysis

Several Python packages have been developed as a part of the Icarus toolkit to aid in the analysis of material response simulations and in particular facilitate applications such as TPS sizing (1-D and multi-dimensional), uncertainty quantification, and sensitivity analysis. The Python package, *icarusPy*, provides utilities for automating common pre-preprocessing and post-processing steps within Icarus. In the analysis presented here, a one-dimensional, material stackup object defined by *icarusPy* is used to automate the creation and setup of all simulations, and a separate simulation management object handles the batching and running of Icarus simulations. These tools are coupled with *uqdriver*, a Python package that provides a customizable interface between a material response code, e.g. Icarus, and several third-party statistical analysis programs such as DAKOTA Adams et al. [2014] or SALib Herman and Usher [2017]. In practical applications, a full analysis might be completed as a series of independent steps, which would involve running *uqdriver* to generate the design of experiments, then running a *icarusPy* simulation manager to generate the material response data, and lastly followed by statistical analysis, which can be facilitated by *uqdriver* program.

Table 1: Uncertainties associated with the material properties of the heatshield DragSTR plugs, adopted from Alpert et al. [2022]. Uniform distributions, $U(L/\mu, U/\mu)$ are defined by the mean-normalized lower and upper bounds, while the normal distributions, $N(2\sigma/\mu)$ are defined by the mean, μ, and standard deviation σ.

Name	Distribution	Parameters
$\rho_v = \rho_c$	$U(L/\mu, U/\mu)$	1 ± 0.018
$C_{v,v} = C_{v,c}$	$N(2\sigma/\mu)$	0.05
$\epsilon_{v,v}$	$N(2\sigma/\mu)$	0.03
$\epsilon_{v,c}$	$N(2\sigma/\mu)$	0.03
$k_{v,v}$	$N(2\sigma/\mu)$	0.12
$k_{v,c}$	Correlated	$(15/12)\, k_{v,v}$

In the present Monte Carlo analysis, representative material stack-ups at the stagnation point and at a shoulder point of the Dragonfly heatshield are selected for analysis to determine the variance in the in-depth location at which the maximum temperature does not exceed 1750 K, the maximum allowable temperature of a type-R thermocouple. The

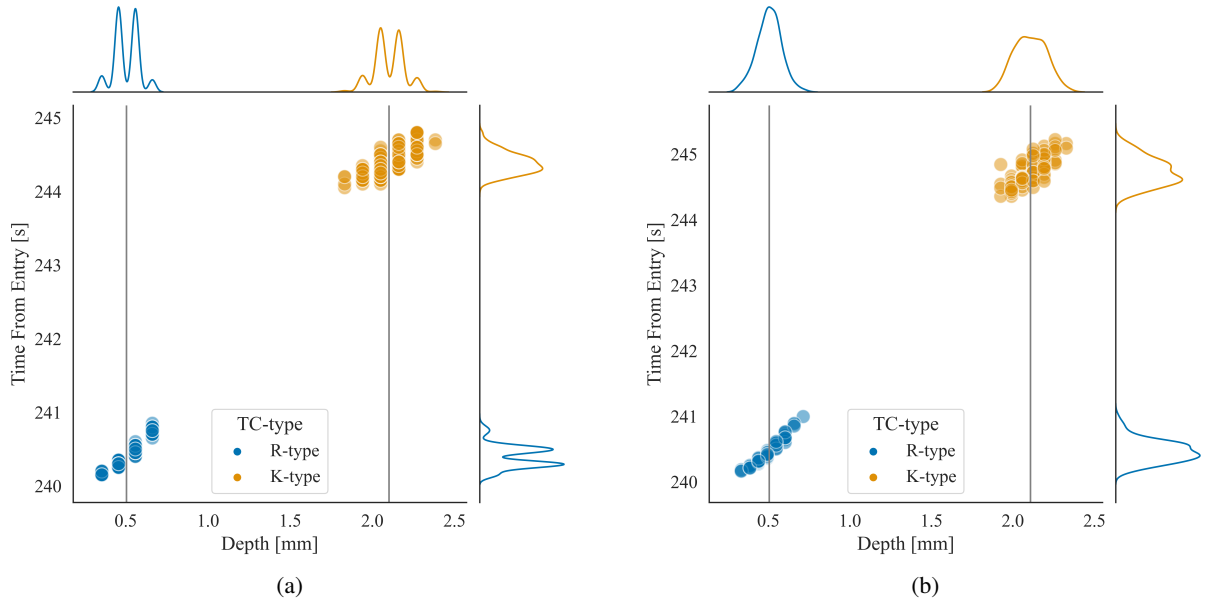

Figure 2: Scatterplot and distributions of the in-depth distances for the temperature exceeds 1750 K (labeled R-type) and 1530 K (labeled K-type). The results are shown for (a) coarse and (b) fine spatial and temporal resolutions. The mean (μ) and standard deviations (σ) in units of millimeters are (a) $\mu_R = 0.504$, $\sigma_R = 0.075$, $\mu_K = 2.102$, $\sigma_K = 0.093$, and (b) $\mu_R = 0.505$, $\sigma_R = 0.073$ and $\mu_K = 2.108$, $\sigma_K = 0.094$.

heatshield material stack-up is primarily composed of PICA and Aluminum-Honeycomb, and the DragSTR plugs in these locations will be composed of PICA and flush-mounted on the aeroshell. To understand the variance of the in-depth material response, the PICA material properties and the surface heating environment (pressure, convective heat flux, and radiative heat flux) are treated as uncertain variables with defined probability distributions. The probability density functions of the virgin and char PICA density, specific heat, thermal conductivity, and surface emissivity are assumed to be similar to those used in a previous analysis of the MELDI2 surface heating reconstructions Alpert et al. [2022]. Those values are reported in Table 1. The surface heating environments are assumed to have a uniform distribution with the lower bounds determined from the best-estimated-trajectory (BET) and the upper bounds determined by the margined environments and are shown in Fig. 1

4 Results

A total of 500 simulations were run, and the inputs to these simulations were generated by sampling the 13 uncertain variable distributions described in Table 1 and Fig. 1 using Latin Hypercube Sampling. Additionally, the Icarus library can be customized to write simulation-specific data files. In this case, the post-processing files contain the locations for the regions within the material where the temperature exceeds 1750 K and 1530 K, the upper temperature limits for R-type and K-type TCs. To account for spatial discretization errors, the location within the mesh at which the temperature is 1750 K or 1530 K is linearly interpolated using the nearest mesh points. For completeness, a one-dimensional stackup consisting of PICA, adhesive, facesheet, and Alumninum honeycomb materials is simulated; however, uncertainties are only applied to the material properties of PICA. Equilibrium properties of the pyrolysis gas products are generated using Mutation Scoggins et al. [2020] using nominal values only. The one-dimensional mesh is hyperbolically-stretched within the PICA layer and remains uniform throughout the remaining materials. The boundary condition given by Eq. 12 is enforced through the simulation at the PICA surface. All other boundaries are considered adiabatic and all internal material interfaces are assumed impermeable, *i.e.*, all pyrolysis gases generated are blown into the boundary layer.

Figure 2(a) shows the distributions and scatterplots of the in-depth distances for the R-type and K-type TCs, which in all the following figures will be meant to refer to the depth at which the temperature exceeds 1750 K and 1530 K, respectively. These data are plotted against the *last* time from entry for which the maximum temperature is exceeded. The mean depth for the R-type TC is approximately 0.5 mm, and the mean depth for the K-type TC is 2.1 mm. The mean values are illustrated on Fig. 2 as reference lines. One immediate observation from these distributions is that they

have a multi-modal form that suggests the statistics are being affected by either the spatial or temporal discretization. For the results in Fig. 2(a), the minimum mesh spacing is 0.1 mm, and at times around at which peak heating occurs, the simulation time step is constant and equal to 0.01 seconds. Even though the collected data are linearly interpolated in space, they are not linearly interpolated in time, and as a result, the data are effectively "binned" according the mesh sizes. To illustrate this, a second batch of 500 simulations was run using a minimum mesh spacing of 0.05 mm and a maximum time step of 0.005 seconds. Figure 2(b) shows the results, and the distributions and scatterplots are more normally distributed about a mean indicating the sensitivity to the temporal discretization. Future analysis will include further data reduction steps by linearly interpolating in time, which should improve the data visualization; however, it is not expected that the mean and standard deviations reported here will be significantly affected.

5 Conclusion

Icarus is a relatively new three-dimensional, unstructured, finite-volume material response solver developed at NASA Ames Research Center Schulz et al. [2017] and has in the last few years reached a level of maturity such that is being used for analysis in many upcoming NASA missions, Dragonfly in particular. One of the objectives of this report is to illustrate some of the mission-relevant capabilities within Icarus. The Monte Carlo analysis presented here demonstrates the utility of several Python packages developed to aid in the analysis of material response simulations. One of the considerations for the DrEAM is the placement and design of the DragSTR plugs. The expected in-depth temperature, as predicted by loosely coupled CFD and material response, dictates the depth of the TCs and potentially the type of TCs used. By running a Monte Carlo analysis of Icarus simulations, the means and variances of the region of in-depth material exceeding 1750 K and 1530 K were computed at the stagnation point. Means values of approximately 0.5 mm and 2.1 mm with standard deviations of 0.073 and 0.094 mm were computed for R-type and K-type TCs respectively. Future analysis will consider other locations on the aeroshell, particularly the shoulder region where the potential for turbulent heating aids additional uncertainty.

6 Acknowledgements

The author would like to thank NASA's Entry Systems Modeling for their support of this work, and the author is supported through the NNA15BB15C contract between NASA Ames Research Center and AMA, Inc.

References

J. Schulz, E. Stern, S. Muppidi, G. Palmer, O. Schroeder, and A. Martian. Development of a three-dimensional, unstructured material response design tool. *AIAA Paper 2017-0667*, 2017. doi:https://doi.org/10.2514/6.2017-0667.

O. Schroeder, J. Brock, E. Stern, and G. Candler. A coupled ablation approach using icarus and us3d. *AIAA Paper 2021-0924*, 2021. doi:https://doi.org/10.2514/6.2021-0924.

A. Brandis, H. Hwang, A. Gulhan, J. Santos, E. Stern, C. Karlgaard, T. Oishi, T. Thiele, F. Siebe, N. Wendel, D. Neeb, and A. Weiss. Overview of the Dragonfly Entry Aerosciences Measurements (DrEAM) Suite. *19th International Planetary Probe Workshop*, 2022.

J. Santos, A. Brandis, H. Hwang, A. Gulhan, T. Thiele, and F. Siebe. Overview of dragonfly entry aerosciences measurements (dream). *2021 Fall Meeting of Outer Planets Assessment Group*, 2021.

H. Hwang, D. Bose, T. White, H. Write, M. Schoenenberger, C. Kuhl, D. Trombetta, J. Santos, T. Oishi, C. Karlgaard, M. Mahzari, and S. Pennington. Mars 2020 entry, descent and landing instrumentation 2 (medli2). *AIAA Paper 2016-3536*, 2013. doi:https://doi.org/10.2514/6.2016-3536.

D. Bose, T. White, M. Mahzari, and K. Edquist. Reconstruction of aerothermal environment and response of mars science laboratory. *Journal of Spacecraft and Rockets*, 51(4), 2013.

H. Alpert, D. Saunders, M. Mahzari, J. Monk, and T. White. Inverse estimation of mars 2020 entry aeroheating environments using medli2 flight data. *AIAA Paper 2022-0550*, 2022. doi:https://doi.org/10.2514/6.2022-0550.

C.B. Moyer and R.A. Rindal. An Analysis of the Coupled Chemically Reaction Boundary Layer and Charring Ablator, Part II, Finite Difference Solution for the In-Depth Response of Charring Materials Considering Surface Chemical and Energy Balances. In *NASA CR-1061*, pages 1–168, June 1968.

A.J. Amar, B.F. Blackwell, and J.R. Edwards. Development and Verification of a One-dimensional Ablation Code Including Pyrolysis Gas Flow. *Journal of Thermophysics and Heat Transfer*, 23(1):59–71, 2009.

F.S. Milos and Y.-K. Chen. Ablation and thermal response property model validation for phenolic impregnated carbon ablator. *Journal of Spacecraft and Rockets*, 47(5):786–805, 2010.

W.J. Adams, B.M. and. Bohnhoff, K.R. Dalbey, M.S. Ebeida, J.P. Eddy, M.S. Eldred, G. Geraci, R.W. Hooper, P.D. Hough, K.T. Hu, J.D. Jakeman, M. Khalil, K.A. Maupin, J.A. Monschke, E.M. Ridgway, A.A. Rushdi, J.A. Stephens, L.P. Swiler, D.M. Vigil, T.M. Wildey, and J.G. Winokur. Dakota, a multilevel parallel object-oriented framework for design optimization, parameter estimation, uncertainty quantification, and sensitivity analysis: Version 6.11 user's manual. *Sandia Technical Report SAND2014-4633*, 2014. updated November 2019.

J. Herman and W. Usher. SALib: An open-source python library for sensitivity analysis. *The Journal of Open Source Software*, 2(9), jan 2017. doi:10.21105/joss.00097. URL `https://doi.org/10.21105/joss.00097`.

J.B. Scoggins, V. Leroy, G. Bellas-Chatzigeorgis, B. Dias, and T. Magin. Mutation++: MUlticomponent Thermodynamic And Transport properties for IONized gases in C++. *SoftwareX*, 12, 2020. doi:https://doi.org/10.1016/j.softx.2020.100575.